

chrome-*c* oxidase is a multiheme protein spanning the mitochondrial membrane of eukaryotic cells that uses electrons transferred from cytoplasmic cytochrome *c* to reduce dioxygen. The protein couples the energy released by this redox chemistry to the transport of protons across the membrane. The heme center which is the site of oxygen binding, cytochrome *a*₃, is similar to Hb and Mb in having a vacant axial binding site distal to the protein that is available to exogenous ligands and a proximal site that is coordinated to the imidazolic nitrogen of a histidine residue. Many time-resolved spectroscopies have been applied to the study of CO photodissociation from this site in an effort to understand the sequence of intraprotein events that culminates in ligand binding and, in the case of O₂, redox chemistry and its mechanistic link to proton pumping. An important component to this understanding is knowledge of the heme iron spin state and axial ligation after ligand photodissociation. Magnetic spectroscopies such as MCD are particularly sensitive to spin state and thus are sensitive to the extent of axial ligation in octahedral Fe complexes.

Although the classic picture of heme protein complexes predicts that cytochrome *a*₃ is pentacoordinate and high spin after CO photodissociation, various lines of evidence called this expectation into question for CcO, particularly time-resolved resonance Raman spectra obtained at very low excitation powers.²⁶ The finding that the TRMCD spectrum of CcO obtained within a few nanoseconds after CO photolysis is similar to the equilibrium MCD spectrum of unliganded CcO (see Fig. 7) unambiguously established the high-spin, pentacoordinate nature of photodissociated cytochrome *a*₃. Reconciling this finding with the resonance Raman evidence, however, led to the inference that an unusual exchange of endogenous axial ligands accompanies binding of exogenous ligands to the distal site.²⁶

[8] Real-Time Spectroscopic Techniques for Probing Conformational Dynamics of Heme Proteins

By ROBERT C. DUNN, XIAOLIANG XIE, and JOHN D. SIMON

Introduction

One of the most thoroughly studied classes of proteins are those that contain heme groups. Heme groups are important in a variety of electron and molecular transport processes. In proteins involved in electron transport reactions, the metal ion complexed by the porphyrin is generally

coordinated to two amino acids. In molecular transport proteins, the metal is usually coordinated by one amino acid; the remaining coordination site is where the molecule being transported by the protein binds. Over the past several decades, there has been an intense effort to understand the factors that control the binding to and subsequent releasing of small molecules from heme proteins. The vast majority of this work has focused on complexes involving myoglobin and hemoglobin.^{1,2} In this chapter, we examine new experimental techniques for studying the protein conformational dynamics that occur on breaking the heme–molecule bond. Because of the immense amount of time-resolved spectroscopic studies that have been reported on heme proteins, the scope of this chapter is limited to dynamics that occur on the picosecond time scale. The reader is referred elsewhere for reviews on slower time dynamics in these and related biological systems.^{1,2}

Before examining the results of various experimental studies, it is instructive to consider what type of motions one might expect heme proteins to undergo on the picosecond time scale associated with ligand loss. For the present purposes, we limit our discussion to the protein myoglobin (Mb), a small protein of 153 amino acids that serves as a reversible oxygen carrier within muscles of vertebrates. The oxygen molecule is bound to an iron-containing heme group, namely, iron(II) protoporphyrin IX. The heme, in turn, is bound to the protein through a covalent bond between the iron and the proximal histidine (F8). The structure of Mb is one of the most carefully characterized among all proteins. The X-ray structure of Mb has been refined to a resolution of 1.5 Å.³ On the basis of the different crystal structures for carbonmonoxymyoglobin (MbCO) and Mb, several protein structural changes are expected on loss of the ligand. These include movement of the iron out of the heme plane, doming of the heme molecule, tilting of the proximal histidine, and displacement of the protein backbone (see Fig. 1). In addition, the spin state of the iron is different in the two structures. Finally, it is known that a fraction of the CO molecules end up diffusing out of the protein into solution.^{4,5} As no obvious path appears from the crystal structure,⁶ there must be fluctuations in the protein structure that open holes large enough for the

¹ R. M. Hochstrasser and C. K. Johnson, in "Ultrashort Laser Pulses and Applications, Topics in Applied Physics" (W. Kaiser, ed.), Vol. 60, p. 357. 1988. Berlin.

² J. Hofrichter, J. H. Sommer, E. R. Henry, and W. A. Eaton, *Proc. Natl. Acad. Sci. U.S.A.* **80**, 2235 (1983).

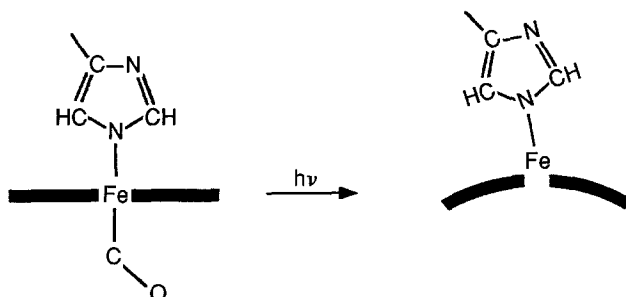
³ J. Kuriyan, S. Wilz, M. Karplus, and G. A. Petsko, *J. Mol. Biol.* **192**, 133 (1986).

⁴ D. A. Duddell, R. J. Morris, and J. T. Richards, *J. Chem. Soc., Chem. Commun.*, 75 (1979).

⁵ J. M. Friedman and K. B. Lyons, *Nature (London)* **284**, 570 (1980).

⁶ C. L. Brooks III, M. Karplus, and B. M. Pettitt, *Adv. Chem. Phys.* **71**, 111 (1988).

Doming of the heme and tilting of the proximal histidine



Displacement of the F-Helix

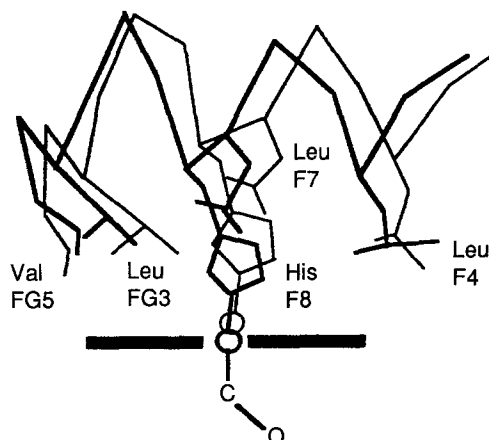


FIG. 1. Structural changes that occur in the vicinity of the heme group following ligand photodissociation.

CO to diffuse out.⁷ In particular, passage of the CO into and out of the heme pocket is thought to involve motions of the distal histidine.⁸ The question at hand is on what time scales do all these various processes occur.

The time scales associated with various dynamic processes that occur after photolysis of MbCO are shown schematically in Fig. 2. This picture

⁷ D. A. Case and M. Karplus, *J. Mol. Biol.* **132**, 343 (1979).

⁸ J. S. Olson, A. J. Mathews, R. J. Rohlfs, K. D. Springer, K. D. Edeberg, S. G. Sligar, J. Tame, J. P. Renaud, and K. Nagai, *Nature (London)* **336**, 265 (1989).

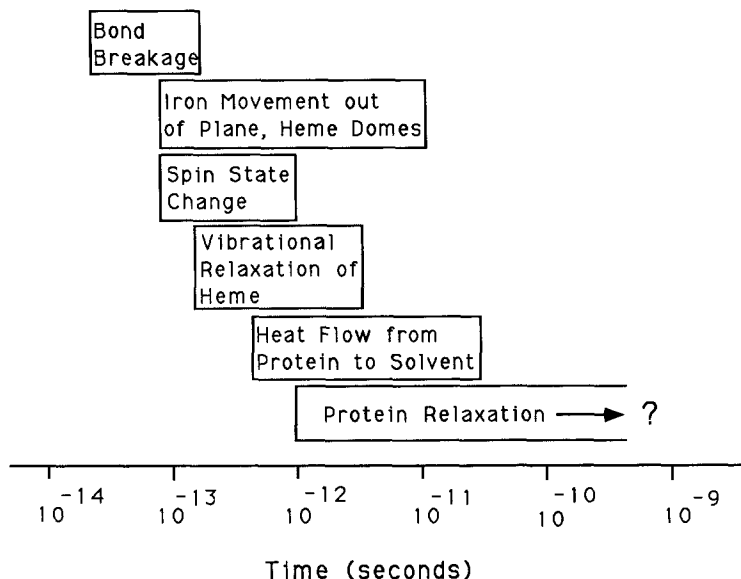


FIG. 2. Time scales for various dynamic processes that occur following the photolysis of MbCO. This general picture of the dynamics has resulted from a combination of many experimental measurements and molecular dynamics simulations. References to individual studies can be found in the text.

has emerged from a combination of many experimental studies⁹⁻¹² and molecular dynamics simulations.¹³ Overall, the combined effort demonstrates that, even in a small protein such as myoglobin, the time required for bond dissociation, vibrational cooling, and subsequent protein structural relaxation spans five orders of magnitude in time. If one includes the diffusion of CO within the protein and finally into the surrounding solution, the time scale range would increase by several orders of magnitude. This diffusional process also requires protein structural fluctuations, which can occur over large time scales. In addition, for many ligands (e.g., O_2 and NO) substantial geminate recombination yields are observed.¹

⁹ B. I. Greene, R. M. Hochstrasser, R. B. Weisman, and W. A. Eaton, *Proc. Natl. Acad. Sci. U.S.A.* **75**, 5255 (1978).

¹⁰ J. L. Martin, A. Migus, C. Poyart, Y. Lecarpentier, R. Astier, and A. Antonetti, *Proc. Natl. Acad. Sci. U.S.A.* **80**, 173 (1983).

¹¹ S. Dasgupta, T. G. Spiro, C. K. Johnson, G. A. Dalickas, and R. M. Hochstrasser, *Biochemistry* **24**, 5295 (1985).

¹² J. N. Moore, P. A. Hansen, and R. M. Hochstrasser, *Proc. Natl. Acad. Sci. U.S.A.* **85**, 5062 (1988).

¹³ E. R. Henry, M. Levitt, and W. A. Eaton, *Proc. Natl. Acad. Sci. U.S.A.* **82**, 2034 (1985).

This process is generally nonexponential and occurs on the hundred picosecond time scale, in competition with many of the relaxation processes indicated in Fig. 2. These observations highlight the complicated nature of protein dynamics. Many complementary experimental techniques are needed to understand fully the wide range of dynamical processes.

Transient Electronic Absorption Spectroscopy

Evolution of the electronic absorption spectrum of heme proteins is extensively used to characterize dynamics associated with ligand photodissociation. The room temperature absorption spectra of Mb and MbCO have been extensively studied.^{14,15} Common features are the Soret band (or B band) at 410–430 nm with an extinction coefficient, ϵ , on the order of $10^5 \text{ cm}^{-1} \text{ M}^{-1}$, the N band centered at 350 nm ($\epsilon \approx 4 \times 10^4 \text{ cm}^{-1} \text{ M}^{-1}$), and the Q band in the region from 520 to 610 nm ($\epsilon \approx 10^4 \text{ cm}^{-1} \text{ M}^{-1}$). All three absorptions correspond to $\pi \rightarrow \pi^*$ transitions centered on the porphyrin ring. In addition to the heme transitions, there are transitions in the UV corresponding to absorptions by various residues in the protein backbone. Buried under these backbone absorptions, in the region below 300 nm, is another heme transition, referred to as the L band. The ligand field $d \rightarrow d$ transitions of the coordinated iron occur in the visible and near-infrared. These transitions, which are significantly weaker than the $\pi \rightarrow \pi^*$ transitions, are not easily observed in the absorption spectrum but have been confirmed by both theoretical calculations and experimental measurements.¹⁶ Finally, charge transfer transitions between the iron and the heme occur in the near-infrared region of the spectrum. These are also generally very weak, exhibiting extinction coefficients on the order of $150 \text{ cm}^{-1} \text{ M}^{-1}$.

Ultrafast laser spectroscopy is frequently used to study the evolution of the Soret and Q bands.^{9,10} As the Soret transition occurs at a different energy in MbCO and Mb, the dynamic evolution of the optical absorption spectrum in this region has been used to establish the time scales associated with photoinitiated ligand loss. The observation that the transient absorption at 300 fsec after excitation is similar to that of equilibrated Mb has been used to establish that ligand loss occurs within a few hundred femtoseconds.¹⁰ The similarity between the transient and equilibrated

¹⁴ W. A. Eaton and J. Hofrichter, this series, Vol. 76, p. 175.

¹⁵ T. Iizuka, H. Yamamoto, M. Kontani, and T. Yonetani, *Biochim. Biophys. Acta* **371**, 126 (1974).

¹⁶ W. A. Eaton, L. K. Hanson, P. J. Stephens, J. C. Sutherland, and J. B. R. Dunn, *J. Am. Chem. Soc.* **100**, 4991 (1978).

spectra has also been used as supportive evidence that the spin-state change occurs on the hundred femtosecond time scale.

The Q band has the unique feature of showing vibrational structure. The lower frequency band, Q_o , is very sensitive to the lifting of the degeneracy of the heme e_{2g} orbitals. As a result, splitting of the Q_{ox} and Q_{oy} bands can be seen in the room temperature absorption band. This suggests that the temporal evolution of this optical absorption provides information on the orbital splitting between x - and y -polarized heme transitions as the protein responds to ligand loss. Careful studies with 30 psec resolution have been reported which establish that the Q band reveals no change in intensity or bandwidth from 30 psec to several nanoseconds following photodissociation.¹⁷

With few exceptions, however, the changes in electronic spectrum do not reveal the conformational dynamics taking place at the heme or in the protein. One exception is the near-infrared charge transfer absorption band of deoxymyoglobin (Mb) and deoxyhemoglobin (Hb).^{18–20} The near-infrared absorption of Mb and Hb, known as band III, occurs at approximately 760 nm. This spectral feature is assigned to a forbidden charge transfer transition ($\epsilon \approx 150 \text{ cm}^{-1} \text{ M}^{-1}$) between the porphyrin π system and the heme iron $a_{2u}(\pi) \rightarrow d_{yz}$.¹⁶ Band III is present only in five-coordinate hemes; low-temperature studies on photodissociated Mb and Hb have shown that the peak position of band III is red-shifted approximately 11 nm in the frozen photoproduct.¹⁵ The position of the peak relaxes to that characteristic of equilibrated Mb or Hb on warming, indicating that unrelaxed intermediates formed immediately after photolysis are trapped at the lower temperatures. These low-temperature studies establish that to some degree band III is sensitive to the structure in the vicinity of the heme iron. As several structural changes occur in the vicinity of the heme on ligand loss, band III has the potential to be a spectroscopic probe of the conformation dynamics of the protein. In principle, band III should be sensitive to movement of the iron out of the heme plate, doming of the heme plate, and tilting of the proximal histidine. The time scale of these movements and the mechanisms controlling them are currently an active area of research.

Band III in both photodissociated Mb and Hb has been studied with nanosecond and subnanosecond resolution at room temperature by many

¹⁷ X. Xie and J. D. Simon, *Biochemistry* **30**, 3682 (1991).

¹⁸ A. Ansari, J. Berendzen, S. F. Bowne, H. Frauenfelder, I. E. T. Iben, T. B. Sauke, E. Shyamsunder, and R. D. Young, *Proc. Natl. Acad. Sci. U.S.A.* **82**, 5000 (1985).

¹⁹ B. F. Campbell, M. R. Chance, and J. L. Friedman, *Science* **238**, 373 (1987).

²⁰ M. D. Chavez, S. H. Courtney, M. R. Chance, D. Kiula, J. Nocek, B. M. Hoffman, J. M. Friedman, and M. R. Ondrias, *Biochemistry* **29**, 4844 (1990).

research groups.^{17,21–23} Work from our laboratory demonstrates that in the case of photodissociated Mb, band III relaxes to its equilibrium value within 35 psec.¹⁷ Recent subpicosecond results from Anfinrud and co-workers establish that band III exhibits dynamics on the few picosecond time scale.²³ Their results show that, immediately on photolysis of Mb, the maximum of band III is red-shifted, in accord with expectations based on the matrix work. This is followed by a spectral evolution of the maximum of band III, which can be correlated to the movement of the iron out of the heme plane. The dynamics of this later event have been calculated from molecular dynamics simulations by Karplus and co-workers.²⁴ Anfinrud and co-workers observe that the spectral evolution of band III quantitatively follows the calculated iron–heme distance.²³ This work provides compelling evidence that the absorption maximum of band III provides a direct measure of the location of the iron with respect to the heme plane. The dynamics observed support the conclusion that the movement of the iron and doming of the heme are complete within a few picoseconds after photodissociation.^{10,13,25}

In contrast, the evolution of band III on photolysis of HbCO exhibits several kinetic processes that last well into the microsecond region.^{21,22} At 35 psec after photodissociating HbCO, the maximum of band III is observed at around 765 nm (see Fig. 3).²² This is red-shifted by 5 nm from that characteristic of equilibrated Hb. In addition, it is interesting to note that this transient feature is blue-shifted from the approximately 770 nm absorption maximum observed in low-temperature matrices.¹⁵ If the matrix spectrum represents the primary structural intermediate formed on photodissociation of HbCO in solution, this suggests that there is a subpicosecond to few picosecond movement of the iron out of the heme plane; however, the protein matrix prevents the iron from moving to the geometry of the equilibrated Hb structure. Although there is some disagreement in the literature about the remaining evolution of band III to equilibrium, our work indicates that no spectral shifts occur between 35 psec and 60 nsec.²² With longer delay times, band III slowly relaxes to its equilibrium value of around 760 nm within a few microseconds.²¹ These results provide interesting insights into the protein dynamics of photogenerated Hb. Whereas the iron–heme geometry relaxes in Mb in tens of picoseconds, microseconds are required in Hb. As each of the

²¹ M. Sassaroli and D. L. Rousseau, *Biochemistry* **26**, 3092 (1987).

²² R. C. Dunn and J. D. Simon, *Biophys. J.* **60**, 884 (1991).

²³ P. Anfinrud, "Proceedings of the Conference on Ultrafast Phenomena VIII." Antibes, France, May, 1992.

²⁴ M. Karplus, personal communication (1992).

²⁵ J. W. Petrich, J. L. Martin, D. Houde, and A. Orszag, *Biochemistry* **26**, 7914 (1987).

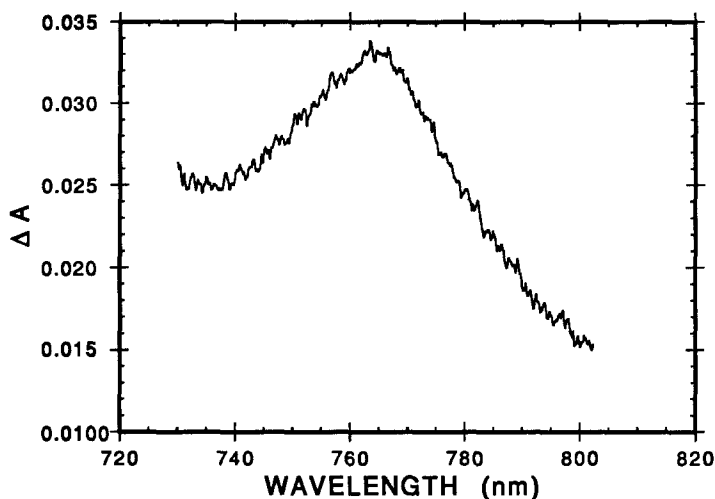


FIG. 3. Transient absorption spectrum of band III at 35 psec following photodissociation of HbCO at 532 nm. The band, centered at 765 nm, is red-shifted 5 nm from that characteristic of equilibrated Hb, indicating the unrelaxed environment of the heme.

four subunits in Hb is similar to those in Mb, this difference in band III dynamics implies that cooperative motions between the subunits are needed for the geometry in the vicinity of the heme to reach equilibrium.

In support of these ideas, theoretical calculations¹³ and recent femto-second transient absorption studies^{10,25} indicate that following photodissociation the initial movement of the iron out of the heme plane occurs within 300 fsec. Longer time evolution in the local structure around the heme group is supported by transient resonance Raman studies on the heme core size marker bands.^{26–28} These vibrations are sensitive to changes in the heme core size, making them diagnostic of displacement of the iron from the plane of the heme. The shifts in these bands reveal a kinetic component that is present 20 nsec after photodissociation, suggesting that the displacement of the iron has a slow component in addition to the subpicosecond process.^{26–28}

Polarization Spectroscopy

Time-resolved polarization spectroscopies are powerful techniques for measuring dynamic motions of biomolecules in solution. Two spectro-

²⁶ J. Turner, J. D. Strong, T. G. Spiro, M. Nagumo, M. Nicol, and M. A. El-Sayed, *Proc. Natl. Acad. Sci. U.S.A.* **78**, 1313 (1981).

²⁷ S. Dasgupta and T. G. Spiro, *Biochemistry* **24**, 5295 (1985).

²⁸ S. Dasgupta and T. G. Spiro, *Biochemistry* **25**, 5941 (1986).

copy techniques that are used measure the linear dichroism (LD)^{12,17,29} and circular dichroism (CD)^{17,29–32} of the sample. Details of nanosecond LD and CD measurements are reviewed by Goldbeck and Kliger elsewhere in this volume.²⁹ They clearly show that these spectroscopic techniques provide important information on biophysical processes that cannot be observed by any other existing experimental techniques.

Linear dichroism with picosecond and subpicosecond time resolution has been available for several years. Many workers have used these techniques to study heme dynamics.^{12,17} The LD data reported have provided insight into the structural dynamics of the heme group following photodissociation as well as the initial motions of the photodissociated ligand in the heme pocket. Most studies to date have probed the time-dependent LD of electronic transitions. Recently, Hochstrasser and co-workers reported an LD technique that probes ground state vibrational transitions of the protein.¹² Using their approach, ligand motions and initial orientations of the CO group in MbCO can be studied. This is an exciting area of new research and is expected to have a large impact on the understanding of protein dynamics in years to come.

Our group has focused on developing techniques for measuring CD signals with picosecond resolution.^{33,34} We have been interested in both natural CD^{17,30,35} as well as that induced in the sample by an external magnetic field (MCD).³⁶ Whereas time-resolved LD measurements probe motions of particular chromophores within the protein, time-resolved CD, in principle, measures changes in the global structure. The remainder of this chapter examines real-time CD spectroscopy on the picosecond time scale. The discussion is organized as follows. First, a brief review of CD is presented. This is followed by a description of the experimental and associated theoretical aspects of performing picosecond time-resolved CD measurements. The last section examines transient CD and MCD results that we have obtained on heme proteins.

²⁹ R. A. Goldbeck and D. S. Kliger, this volume [7].

³⁰ R. C. Dunn and J. D. Simon, in "Proceedings of the International Conference on Lasers '90," STS Press, McLean, Virginia, 1991.

³¹ J. W. Lewis, R. F. Tilton, C. M. Einterz, S. J. Milder, I. D. Kuntz, and D. S. Kliger, *J. Phys. Chem.* **89**, 289 (1985).

³² S. J. Milder, S. C. Bjorling, I. D. Kuntz, and D. S. Kliger, *Biophys. J.* **53**, 659 (1988).

³³ X. Xie and J. D. Simon, *Opt. Commun.* **69**, 303 (1989).

³⁴ X. Xie and J. D. Simon, *Rev. Sci. Instrum.* **60**, 2614 (1989); X. Xie and J. D. Simon, *Proc. SPIE—Int. Soc. Opt. Eng.* **1204**, 66 (1990).

³⁵ X. Xie and D. Simon, *Biochim. Biophys. Acta* **1057**, 131 (1991).

³⁶ X. Xie and J. D. Simon, *J. Phys. Chem.* **94**, 8014 (1990).

Circular Dichroism

Chiral molecules (C_n and D_n symmetry groups) can exhibit preferential absorption of left or right circularly polarized light. This preferential absorption is termed circular dichroism (CD) and is quantified by the difference in extinction coefficient for the left and right circularly polarized light [Eq. (1)]. A quantum mechanical formulation of CD involves calculation

$$\Delta\epsilon = \epsilon_l - \epsilon_r \quad (1)$$

of a quantity called the rotational strength, R . The rotational strength of a transition from state Ψ_1 to Ψ_2 is proportional to the integral shown in Eq. (2), where $\hat{\mu}_{el}$ and $\hat{\mu}_m$ are the electronic and magnetic transition

$$R_{1\rightarrow 2} \propto [\int \Psi_1 \hat{\mu}_{el} \Psi_2 d\tau][\int \Psi_1 \hat{\mu}_m \Psi_2 d\tau] \quad (2)$$

dipole moments, respectively. The CD (quantified by $\Delta\epsilon$) signal is related to the rotational strength through Eq. (3), where h is Planck's constant,

$$R_{1\rightarrow 2} \propto (hc/N_A) \int [\Delta\epsilon(\lambda)]/\lambda d\lambda \quad (3)$$

c is the speed of light, and N_A is Avogadro's number. As can be seen from Eqs. (2) and (3), CD arises from a projection of the electronic dipole transition moment on the corresponding magnetic dipole transmission moment. CD is therefore observable only at wavelengths where there are electronic transitions in the molecule. The signal can be either positive or negative in sign and is usually very weak, with $\Delta\epsilon/\epsilon$ ratios of 10^{-3} to 10^{-6} . A complete discussion of CD and MCD can be found elsewhere.³⁷

In proteins, the CD signal arising from the backbone structure has distinctive characteristics in the region from 200 to 300 nm. Protein UV CD data are used extensively to determinate the proportions of various types of secondary structure in the overall three-dimensional structure. In heme proteins, in addition to the backbone CD signals in the UV, there are CD bands in the UV-visible and near-infrared regions corresponding to the heme $\pi \rightarrow \pi^*$ electronic transitions.

Theoretical calculations of the CD spectra of Mb (and Hb) based on the known three-dimensional structure were first reported by Hsu and Woody.³⁸ This work established that the origin of the optical activity for heme transitions arose from a coupled oscillator interaction between the $\pi \rightarrow \pi^*$ transitions on the heme and those of the surrounding aromatic

³⁷ W. C. Johnson, *Proteins—Structure, Function, and Genetics* **7**, 205 (1990).

³⁸ M.-C. Hsu and R. W. Woody, *J. Am. Chem. Soc.* **93**, 3515 (1971); M.-C. Hsu and R. W. Woody, *J. Am. Chem. Soc.* **91**, 3679 (1969); R. Woody, in "Biochemical and Clinical Aspects of Hemoglobin Abnormalities." Academic Press, New York, 1978.

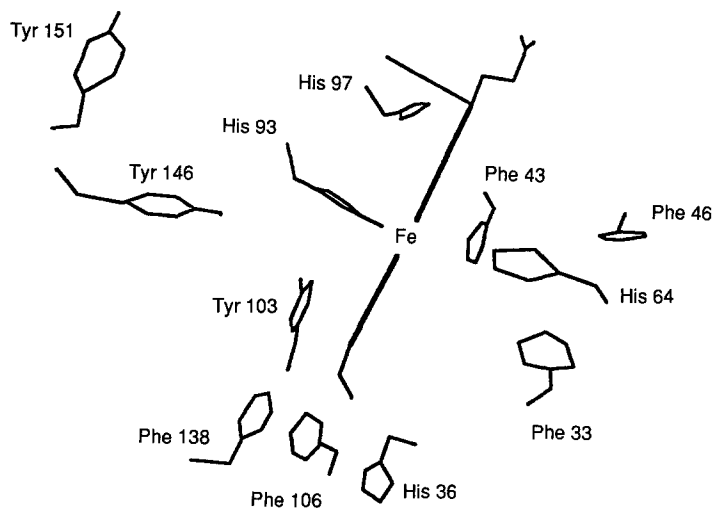


FIG. 4. Orientations of the aromatic amino acids that cause the circular dichroic properties of the heme optical transitions. The rotational strengths derived from the individual amino acids are given in Table I.³⁸

side chains. These calculations indicated that aromatic residues as far as 12 Å away from the heme contribute appreciably to the CD spectrum.

The calculations by Hsu and Woody³⁸ were based on the extension by Tinoco³⁹ of the Kirkwood theory.⁴⁰ The underlying assumption of Kirkwood theory is that the molecule can be divided into N smaller groups, where there is no charge transfer between the various groups. Within this model, the rotational strength entails calculation of the cross-products of the electric transition dipole moments of the heme with electrically allowed transitions of surrounding aromatic residues and dot products of the heme electronic transition dipole with the magnetic transition dipoles of the aromatic residues. The transition dipole moments and transition frequencies can be obtained from either spectroscopic measurements or molecular orbital calculations. The interaction potential between the transition dipole moment of the heme and that of the transition dipoles of the aromatic residues, in a point monopole approximation,^{38,39} can be calculated with knowledge of the wave functions of the two molecular states involved.

The aromatic amino acids that contribute to the optical activity of the heme are shown in Fig. 4. The calculated rotational strengths for these amino acids, as well as their distances from the heme ring, are given in

³⁹ I. Tinoco, Jr., *Adv. Chem. Phys.* **4**, 113 (1962).

⁴⁰ J. G. Kirkwood, *J. Chem. Phys.* **5**, 479 (1937).

TABLE I
CALCULATED ROTATIONAL STRENGTHS OF HEME TRANSITIONS IN MYOGLOBIN^a

Amino acid	Distance (Å)	Porphyrin transition			
		Soret		Q	N
		R_x	R_y	$R_x + R_y$	$R_x + R_y$
His(36,1C)	14.3	-0.080	0.060	0.0003	-0.0055
His(64,7F)	4.7	0.248	-0.426	-0.0018	-0.0056
His(93,8F)	3.6	0.417	-0.393	0.0001	0.0047
His(97,2FG)	6.5	0.068	-0.169	0.0017	0.0044
Phe(33,14B)	6.7	0.106	0.1060	0.0015	0.0121
Phe(43,1CD)	5.9	0.261	-0.217	0.0120	-0.0411
Phe(46,4CD)	9.9	-0.093	0.142	0.0001	0.0070
Phe(106,7G)	14.3	-0.089	0.033	0.0003	-0.0094
Phe(138,15H)	9.6	0.033	0.045	0.0008	0.0049
Tyr(103,4G)	11.3	0.252	-0.004	-0.0005	0.0328
Tyr(146,23H)	11.8	0.135	-0.234	0.0001	-0.0123
Tyr(151,2HC)	15.3	0.037	0.014	0.0000	0.0030
Subtotal		1.295	-0.989		
Total			0.306	0.0146	-0.0050

^a Arising from interaction between heme electronic states and allowed $\pi \rightarrow \pi^*$ transitions in aromatic side chains. All rotational strengths are in units of Debye-Bohr magnetons. Distances are between the centers of the aromatic side chains and the heme. These results are reproduced from the work of Hsu and Woody.³⁸

Table I.³⁸ The dominant contributions to the CD spectrum come from interactions between the heme and Phe(33,14B), Phe(43,1CD), Tyr(103,4G), and Tyr(146,23H). Interactions with the proximal and distal histidines, His(93,8F) and His(64,7F), respectively, are much smaller. It is important to note that the CD spectrum is influenced by amino acids contained in regions of the protein that are not located near the covalent bond between the heme iron and the amino acid backbone. Thus, unlike the case for many of the spectroscopic probes discussed above, temporal evolution of CD signals will provide information on conformational changes in the overall protein structure around the heme ring.

Experimental Designs

As of the writing of this chapter, our group is the only one measuring CD signals in proteins with picosecond resolution. Because of this, a brief description of the methodology used to collect picosecond CD data is appropriate.

The majority of steady-state CD spectrometers in use today are based on the technique of polarization modulation.^{41,42} In this method a linearly polarized beam of light is modulated by a birefringent crystal to produce light whose polarization properties oscillate between $+\frac{1}{4}$ and $-\frac{1}{4}$ wave retardation at a well-defined frequency. This modulated beam is then sent through a chiral sample. The sample preferentially absorbs one of the circularly polarized components of the incident light. The difference between transmission of the two circularly polarized beams is easily determined using phase-sensitive detection that is referenced to the modulation frequency. Because this method is based on the absorptive properties of the sample, it is free from many of the birefringence-associated artifacts inherent in ellipsometric measurements. In addition, present-day photoelastic modulators can be driven at high frequencies (~ 100 kHz range), improving the signal-to-noise ratios and reducing the problems associated with lamp intensity fluctuations.

The polarization modulation technique has been used to record CD signals with millisecond time resolution.^{43,44} In principle, the time resolution could be extended to that corresponding to a single oscillation of the modulator, providing nearly microsecond resolution. However, the technical limitations in the driver frequency for photoelastic modulators suggested that this technique was not amenable to submicrosecond spectroscopy. The feasibility of performing CD measurements in this faster (submicrosecond) time regime was first demonstrated by Kliger and co-workers.^{31,45,46} As detailed elsewhere in this volume,²⁹ these workers are able to collect CD signals on the nanosecond time scale using an ellipsometric measurement. With the development of stable, high repetition rate picosecond laser systems, it became apparent to us that the general concept of polarization modulation and phase-sensitive detection could be used to develop CD spectroscopy in the ultrafast time domain.

A schematic of the experimental apparatus developed to collect picosecond CD spectra is shown in Fig. 5.^{33,34} This method utilizes a high repetition rate laser system (1 kHz) capable of producing tunable picosecond (40 psec) pulses throughout the UV, visible, and near-infrared spectral region ($205 < \lambda < 950$ nm).³³ The purpose of the present discussion is to

⁴¹ L. Velluz, M. Legrand, and M. Grosjean, "Optical Circular Dichroism." Verlag Chemie, New York, 1965.

⁴² A. F. Drake, *J. Phys. E: Sci. Instrum.* **E-30**, 170 (1986).

⁴³ P. M. Bayley and M. Anson, *Biopolymers* **13**, 401 (1974).

⁴⁴ F. A. Ferrone, J. J. Hopfield, and S. E. Schnatterly, *Rev. Sci. Instrum.* **45**, 1392 (1974).

⁴⁵ C. M. Einterz, J. W. Lewis, S. J. Milder, and D. S. Kliger, *J. Phys. Chem.* **89**, 3845 (1985).

⁴⁶ D. S. Kliger and J. W. Lewis, *Rev. Chem. Intermed.* **8**, 367 (1987).

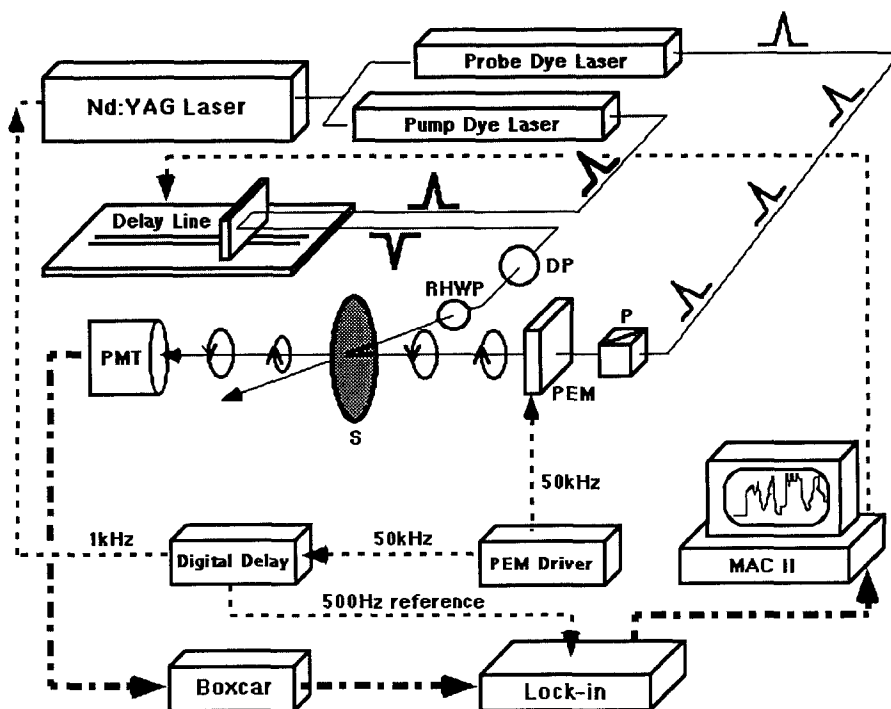


FIG. 5. Schematic of the experimental arrangement used to collect picosecond CD data. A mode-locked, Q-switched Nd-YAG laser operating at 1 kHz is used to synchronously pump two tunable cavity-dumped dye lasers. The output pulses from the pump dye laser are sent through an optical delay line, depolarizer (DP), and rotating half-wave plate (RHWP) before traversing the sample. The change in CD of the sample following excitation with a pump pulse is measured using pulses from the probe dye laser. These pulses are passed through a polarizer (P) and a photoelastic modulator (PEM) operating at 50 kHz. With $\pm\frac{1}{4}$ retardation set on the PEM, the emerging pulse train consists of alternating circularly polarized pulses. These pulses are directed through the sample and detected with a photomultiplier tube (PMT). The output of the PMT is sent to a boxcar and then fed into a lock-in amplifier referenced to the modulation rate (500 Hz) of the pulses out of the PEM. The CD detected by the lock-in amplifier is recorded on a MAC II computer, which also controls the delay line. The synchronization between the retardation on the PEM crystal and the probe pulses is achieved with the use of a digital delay generator. The 50 kHz signal used to drive the PEM crystal is counted down to 1 kHz in the digital delay box and used to control the firing of the laser system.

present the general experimental methodology. Detailed descriptions of the laser system and electronics can be found elsewhere.^{33,34}

An acoustooptically mode-locked and Q-switched neodymium-yttrium-aluminum-garnet (Nd-YAG) laser synchronously pumps two

electrooptically cavity-dumped dye lasers.³³ The output pulses from the two dye lasers are used to generate the pump and probe pulses for the time-resolved measurements. In a pump-probe experimental arrangement, an intense pump pulse is used to perturb the sample of interest (i.e., photodissociate the ligand in myoglobin and hemoglobin), after which a probe light pulse follows at fixed time delays to measure the response of the sample to the perturbation. In our experimental arrangement, the probe pulses are used to determine the transient CD in the sample. This is accomplished by sending the output pulses from the probe dye laser through a linear polarizer followed by a photoelastic modulator.³⁴ The linear polarizer defines the polarization axis of the experiment. The photoelastic modulator is timed to the laser system, providing the means for generating an oscillating train of left and right circularly polarized light pulses at a frequency of 500 Hz (half the repetition rate of the laser). This polarization-modulated pulse train is passed through the sample and detected. The key to this approach lies in the coupling of a photoelastic modulator to the laser system. Whereas the steady-state spectrometer passes a continuous beam through the sample that is evolving in its polarization properties, the picosecond device delivers pulses of light to the sample that pass through the modulator when it is at precisely $+\frac{1}{4}$ and $-\frac{1}{4}$ wave retardation.

As shown in Fig. 5, the output of the photoelastic modulator driver (operating at 50 kHz) is sent to a pulse delay generator. The signal from the modulator is counted down in the delay box to 1 kHz and used to control the firing of the laser system. This allows for a synchronization between the laser pulses and the retardation on the modulator, providing complete control of the probe pulse polarization. For CD measurements, the retardation voltage on the photoelastic modulator is set for $\pm\frac{1}{4}$ wave retardation, alternating the probe pulses sequentially between left and right circular polarizations. For LD measurements, the modulator can be set to $\pm\frac{1}{2}$ wave retardation, providing probe pulses which alternate between parallel and perpendicular polarizations. It is important to note that by using the modulator to trigger the laser system, the ultimate time resolution for this arrangement is limited only by the laser pulse width, not the modulation frequency of the retarder.

Once passed through the sample, the probe pulses are detected with an end-on photomultiplier tube (PMT). Intensity fluctuations inherent in ultrafast lasers result in a pulse-to-pulse amplitude instability of approximately 5%. CD signals from the sample result in an attenuation of the modulated pulse amplitude by less than 0.1%. This illustrates the challenge in performing CD measurements with picosecond time resolution. To extract the small CD signals buried in the large-intensity fluctuations of

the laser system, a combination of phase-sensitive detection and track-and-hold circuits is employed.³⁴

A phase-sensitive detector (lock-in amplifier) can be thought of as a band pass filter which detects only those signals that are modulated at the frequency to which it is referenced. The width of the filter is inversely proportional to the time constant used. It is possible to show that the signal amplitude can be expressed as a Fourier series expansion [Eq. (4)],

$$f(t) = 0.5a_0 + \sum a_n \cos(n\omega t + \phi) \quad (4)$$

where ω is the modulation frequency and ϕ is the phase shift. By assuming rectangular pulses, the amplitude, a_f , of the signal at the reference frequency is given by Eq. (5), where ΔV is the voltage difference arising

$$a_f = (2\Delta V/\pi) \sin(\pi\tau/2L) \quad (5)$$

from the CD signal (\sim mV), τ is the pulse duration (5 nsec out of the PMT), and L is the time between pulses (1 msec). The resulting calculated amplitude is on the order of nanovolts, which is beyond the limits of a lock-in amplifier given the laser pulse intensity fluctuations. A solution to this dilemma involves using track-and-hold circuits to increase the duty cycle.³⁴ In this arrangement, the amplified output of the PMT is fed directly into the track-and-hold circuit, which outputs a nearly perfect square wave with $\tau \approx L$. This signal is then sent to the lock-in amplifier, where, in the limit of a perfect square wave, a maximum amplitude equal to $2\Delta V/\pi$ is seen. In this limit, the shape of the signal is the same as that used in conventional CD spectrometers, and the maximum signal amplitude detected by the lock-in amplifier is on the order of millivolts. In principle, the picosecond device should be able to measure CD signals that are comparable to those obtained on steady-state machines.

Jones Matrix Analysis

Measurements of CD signals are complicated by the fact that they are inherently small signals susceptible to artifacts that arise from the birefringence of the optics and sample. The similarity between the steady-state and time-resolved techniques suggests that methods used in conventional spectroscopy to reduce these effects will also be appropriate for the picosecond spectroscopy. However, in the time-resolved experiments, further complications arise from pump-induced polarization effects in the sample. To appreciate fully the influence of the pump beam on the observed signals it is necessary to model the polarization properties of the light as it traverses the optical path of the experiment. It is clear that excitation by polarized light results in a photoselection in the sample.

This, in turn, give rises to a birefringence which exhibits complicated dynamics that are tied to the rotational tumblings and excited state lifetimes of the molecules being studied. These effects need to be minimized, so that the CD properties can be isolated and measured. In minimizing these unwanted polarization effects, it is important not to diminish the desired CD signal. Thus, a careful modeling of the experimental design is essential.

Fortunately, polarized light experiments can be conveniently modeled using Jones matrix calculus.^{47,48} This enables a complete description of the polarization properties of the light at each step in the experiment. A comprehensive Jones matrix analysis of the picosecond CD experiment detailing the potential sources of artifacts has appeared.⁴⁹ Here we examine a few of the details and consider the physical principles by which the CD signal is isolated and measured.

The procedure for using Jones matrices to describe the polarization of the light is conceptually straightforward. If one assumes that the light is traveling in the z direction, then the polarization of the light in the x, y plane can be described by a column matrix (**J** matrix) containing two elements. The functional forms of the elements in the **J** matrix depend on the polarization of the light.

The effect an optical element in the experiment can have on the polarization of the incoming light can be described by a 2×2 matrix (commonly called an **M** matrix). The functional forms of the elements in these matrices depend on the type of effect being described (linear birefringence, circular birefringence, etc.) and are well known.⁴⁸ Matrix multiplication of the **J** matrix with the **M** matrix (matrices), in the order in which the light will pass through them, gives a resulting column matrix which describes the polarization properties of the exiting light beam. In practice, optical elements or samples often exhibit more than one polarization-altering property. For example, a sample that exhibits CD could also be linearly birefringent. This complicates the above analysis, as the matrices describing these individual processes do not commute with each other. This problem is handled using an expansion technique known as the N -matrix calculus. The details of this approach can be found in the literature.⁴⁷⁻⁴⁹ This type of analysis is required to determine the combined effects of circular birefringence, linear birefringence, and linear dichroism associated with the photolysis of samples in the picosecond CD experiment.⁴⁹

⁴⁷ R. C. Jones, *Opt. Soc. Am.* **31**, 488 (1941); **31**, 493 (1941); **31**, 500 (1941); **32**, 486 (1942); **37**, 107 (1947); **37**, 110 (1947); **38**, 671 (1948).

⁴⁸ D. S. Kliger, J. W. Lewis, and C. E. Randall, "Polarized Light in Optics and Spectroscopy." Academic Press, Boston, 1990.

⁴⁹ X. Xie and J. D. Simon, *J. Opt. Soc. Am. B* **7**, 1673 (1990).

We can gain physical insight into the problems and possible cures of unwanted pump-induced polarization signals by considering the case where these effects are maximized. In the experimental apparatus, the ratio of the difference in transmitted intensities is measured to the direct current (dc) signal: $(E_L^2 - E_R^2)/(E_L^2 + E_R^2)$. In terms of the optical calculus, the detected signal is given by Eq. (6), where b is the retardation

$$\frac{E_L^2 - E_R^2}{E_L^2 + E_R^2} = CD f(\rho, b, \theta) + LD g(b, \theta) \quad (6)$$

angle of the linear birefringence of the sample, ρ is the retardation angle resulting from the pump-induced linear birefringence, θ is the angle of the fast axis of the optic with respect to the polarization axis of the pump beam, and CD and LD are the circular dichroism and linear dichroism signals. Thus, excitation by a polarized pump laser results in a signal which contains components of both the linear and circular dichroism of the sample. As the LD is generally orders of magnitude more intense than the CD , the signal is dominated by the LD component. Solution to this problem becomes apparent from the functional forms of $f(\rho, b, \theta)$ and $g(b, \theta)$. By modulating θ at a frequency different from that used to detect the CD , the LD and CD components can be discriminated by the lock-in detection.⁴⁹ Experimentally this is accomplished by spinning a half-wave plate in the excitation beam at a frequency of 3.5 Hz. This modulates the LD at 7 Hz. The CD is modulated at half the laser repetition rate (500 Hz). By using an appropriate time constant, the lock-in amplifier easily distinguishes these signals, and complete suppression of the LD contributions is obtained.^{34,49}

Picosecond Circular Dichroism Studies of Heme Proteins

Myoglobin

The first-time resolved CD studies of the photolysis of MbCO were reported by Lewis *et al.*³¹ and Milder *et al.*³² The CD values at several absorption wavelengths changed from that expected for MbCO to that of Mb within a few nanoseconds (the resolution of the experiment). No evolution in signals was observed for several hundred nanoseconds, indicating that the protein was relaxing on the picosecond time scale. In Fig. 6, the picosecond evolution of the CD signal probed near the peak of the N-band absorption (λ 355 nm) is plotted as a function of time following photolysis.¹⁷ The dashed line is a normalized transient absorption signal for the same sample at the same wavelength, providing a measure of the

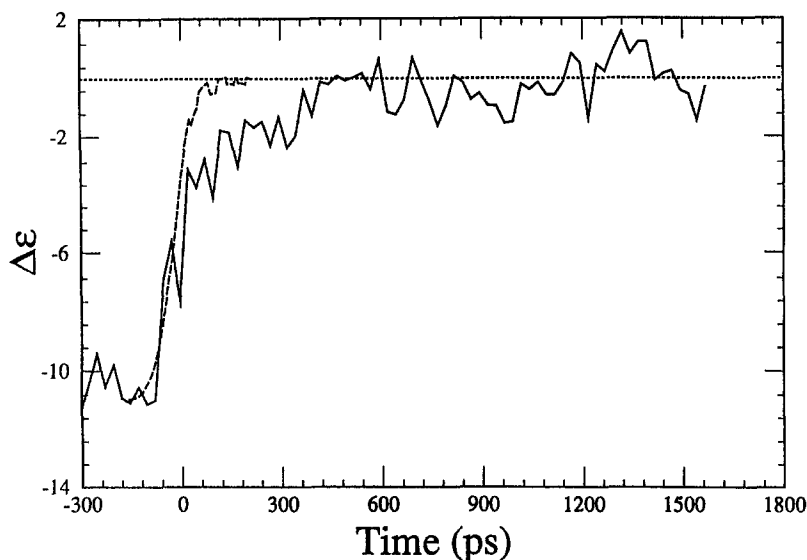


FIG. 6. Transient circular dichroism kinetics of Mb probed at 355 nm following photodissociation of CO (solid line). The dashed line is the normalized transient absorption signal recorded at the same wavelength, and the dotted line is the equilibrium CD value for Mb. The transient CD trace reveals two kinetic processes. The instantaneous component is due to the electronic state change that occurs on photodissociation. The longer relaxation time reflects conformational changes in the surrounding protein structure.

instrument response. The CD signals observed prior to photolysis and at long times ($t > \text{nsec}$) are consistent with the steady-state CD values of MbCO and Mb at 355 nm, respectively. The important observation from these data is that the evolution of the CD signal is distinctly different from the transient absorption kinetics.

The picosecond CD data exhibit two major components. Approximately half of the observed signal change occurs within the instrument response. This is followed by a slower rise reflecting a relaxation process that is approximately two orders of magnitude slower than the dynamics of photoinduced bond cleavage ($\sim 200\text{--}300 \text{ fsec}$). The instantaneous change in the CD signal following photolysis has been interpreted in terms of the electronic state change of the heme group that accompanies the change from six- to five-coordinate iron.¹⁷

Several possible models can be invoked to account for the dynamic changes in the CD signal that are observed on the hundred picosecond time scale. Three molecular mechanisms consistent with the observed data are vibrational relaxation in the vicinity of the heme, time-dependent splitting of the degeneracy of the heme transitions, and relaxation of the

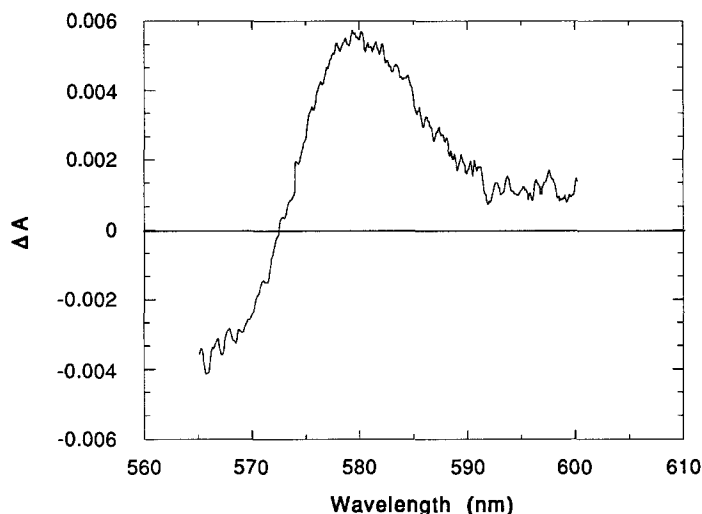


FIG. 7. Steady-state MCD spectrum of the Q-band transition of MbCO. The spectrum was recorded using the picosecond apparatus, blocking the excitation beam.

surrounding protein matrix. Phase-grating experiments of Miller and co-workers⁵⁰ reveal that vibrational relaxation in the vicinity of the heme is complete within 25 psec, significantly faster than the relaxation process revealed by the CD data. To address the possibility of a time-dependent splitting in the degeneracy of the heme transitions, the following experiments were performed: (1) picosecond linear dichroism studies on the Soret absorption bands and (2) detailed time-resolved absorption studies of the Q band. The details of these studies are reported in the literature.^{17,36} They reveal no evidence for a time-dependent splitting of the degeneracy of the heme transitions. Thus, combined with detailed spectroscopic studies and a variety of time-resolved linear dichroism experiments, the evolution of the CD signal for several hundred picoseconds is revealing information on the relaxation of the protein structure in response to deligation.

Based on the calculations reported by Hsu and Woody,³⁸ the CD of the N band of Mb depends on the orientations of aromatic residues as far away as 12 Å from the heme. Although the exact motions that give rise to the dynamics cannot be assigned at this time, the results suggests that time-resolved CD can be useful in probing the dynamics of protein

⁵⁰ L. Genberg, F. Heisel, G. McLendon, and R. J. D. Miller, *J. Phys. Chem.* **91**, 5521 (1987); L. Genberg, Q. Bao, S. Gracewskiz, and R. J. D. Miller, *Chem. Phys.* **31**, 81 (1989); L. Genberg, L. Richard, G. McLendon, and R. J. D. Miller, *Science* **251**, 1051 (1990).

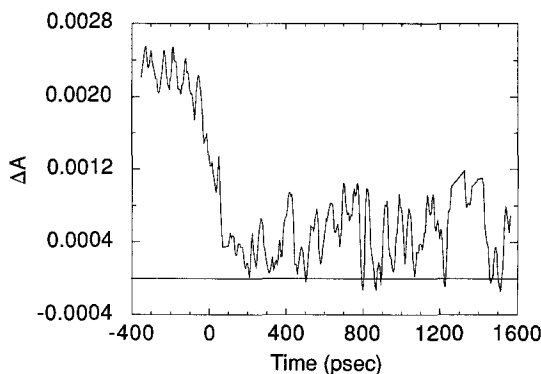


FIG. 8. Time-resolved MCD signal at 580 nm following the photodissociation of MbCO at 532 nm. At $t = 0$ the signal drops from that characteristic of a low-spin iron to that reflective of a high-spin metal. The signal remains constant for 1 nsec, suggesting that there are no dynamic changes in the heme structure on this time scale.

structural changes that occur outside the immediate environment of the heme group.

One particular molecular motion that could account for the evolution of the CD signal involves the tilting of the proximal histidine. It is worth noting that the importance of this motion can be independently addressed by examining the dynamics of band III. As described above, a detailed dynamic study of this absorption band reveals no change in band shape or band position from 20 psec (the instrument response) to 10 nsec following photodissociation.¹⁷ The absorption maximum is that observed for equilibrium myoglobin. This result suggests that the tilting of the proximal histidine as well as other structural changes that contribute to the shape and maximum of band III are not responsible for the observed CD kinetics.

To address further the time scale on which the iron goes from low to high spin following CO elimination, picosecond MCD dynamics of the Q_o band of Mb were examined.³⁶ The Q band was chosen because the MCD of this transition is very sensitive to changes in the spin state of the iron and the geometry of the heme group.⁵¹ In comparing Mb (high spin) to MbCO (low spin), the signal decreases by approximately a factor of five. The MCD spectrum of the Q band for MbCO shown in Fig. 7 was collected on the picosecond spectrometer with the photolysis beam blocked. The

⁵¹ J. C. Sutherland and B. Holmquist, *Annu. Rev. Biophys. Bioeng.* **9**, 293 (1980); B. Holmquist, this series, Vol. 130, p. 270; A. D. Buckingham and P. J. Stephens, *Annu. Rev. Phys. Chem.* **17**, 399 (1966); P. N. Schatz and A. J. McCaffery, *Q. Rev. Chem. Soc.* **23**, 552 (1969); R. A. Goldbeck, *Acc. Chem. Res.* **21**, 95 (1988); P. J. Stephens, *Annu. Rev. Phys. Chem.* **25**, 201 (1974).

time-dependent MCD change at 580 nm following dissociation is shown in Fig. 8. The MCD signal drops to nearly zero within the instrument response. Two important observations are obtained from these results. First, the change of spin state in Mb occurs within the time resolution of the measurements. This provides supporting evidence for the conclusion drawn from ultrafast absorption spectroscopy¹⁰ that the spin-state change occurs on the subpicosecond time scale. Second, within the limitations of the signal-to-noise ratio of the experiments, there is no detectable evolution of the electronic structure of the heme group from 30 psec to several nanoseconds following dissociation. This result is consistent with detailed measurements on the time evolution of the shape of the Q-band absorption.⁷

Hemoglobin

We have carried out time-resolved CD experiments on HbCO³⁰ aimed at addressing questions that were raised by the dynamics observed for band III. In particular, to investigate what structural processes are responsible for the subpicosecond relaxation in Hb that shifts band III from approximately 770 nm observed in the matrix to 765 nm which we observe at 35 psec,²² time-resolved circular dichroism measurements of the 266 nm band were made. Although in the aromatic region of the spectrum, this band is known to be a sensitive marker of the change in the iron(III) from that of low spin to high spin following photolysis.³⁸ The CD signal evolves from that characteristic of HbCO to that expected for equilibrated Hb within the instrument response of 80 psec. This results indicates that the spin-state change is occurring on a faster time scale, consistent with the subpicosecond movement of the iron(III) out of the heme plane inferred from the band III measurements. This agrees with calculations¹³ and experiments¹⁰ indicating that the initial movement of the iron takes less than a couple hundred femtoseconds. This subpicosecond movement is likely responsible for the ultrafast shift that takes band III from 770 nm observed in the matrix to 765 nm observed at 35 psec; however, femtosecond measurements are needed to confirm this conclusion.

Acknowledgments

The work described in this chapter is supported by the National Institutes of Health through Grant GM-41942 and the Materials and Medical Free Electron Laser (MMFEL) Program administered by the Office of Naval Research.